



Article

Chemo-Enzymatic Synthesis of Renewable Sterically-Hindered Phenolic Antioxidants with Tunable Polarity from Lignocellulose and Vegetal Oil Components

Louis Hollande ^{1,2}, Sandra Domenek ² and Florent Allais ^{1,*}

¹ Chaire ABI, AgroParisTech, CEBB 3 rue des Rouges Terres 51110 Pomacle, France; louis.hollande@agroparistech.fr

² UMR GENIAL, AgroParisTech, INRA, Université Paris-Saclay, Avenue des Olympiades, 91300 Massy, France; sandra.domenek@agroparistech.fr

* Correspondence: florent.allais@agroparistech.fr

Received: 28 September 2018; Accepted: 24 October 2018; Published: 26 October 2018



Abstract: Despite their great antioxidant activities, the use of natural phenols as antioxidant additives for polyolefins is limited owing to their weak thermal stability and hydrophilic character. Herein, we report a sustainable chemo-enzymatic synthesis of renewable lipophilic antioxidants specifically designed to overcome these restrictions using naturally occurring ferulic acid (found in lignocellulose) and vegetal oils (i.e., lauric, palmitic, stearic acids, and glycerol) as starting materials. A predictive Hansen and Hildebrand parameters-based approach was used to tailor the polarity of newly designed structures. A specific affinity of *Candida antarctica* lipase B (CAL-B) towards glycerol was demonstrated and exploited to efficiently synthesize the target compounds in yields ranging from 81 to 87%. Antiradical activity as well as radical scavenging behavior (H atom-donation, kinetics) of these new fully biobased additives were found superior to that of well-established, commercially available fossil-based antioxidants such as Irganox 1010[®] and Irganox 1076[®]. Finally, their greater thermal stabilities (302 < T_d5% < 311 °C), established using thermal gravimetric analysis, combined with their high solubilities and antioxidant activities, make these novel sustainable phenolics a very attractive alternative to current fossil-based antioxidant additives in polyolefins.

Keywords: ferulic acid; fatty acid ethyl esters; CAL-B; antioxidant; DPPH

1. Introduction

In contact with atmospheric oxygen, polymers undergo oxidative degradation reactions during fabrication processes, storage, and throughout their use [1–4]. Involving undesirable radical species (R•) and mechanisms, these oxidative degradation reactions drastically impact the initial aesthetic and mechanical properties of the polymers [1,5,6]. This ineluctable phenomenon is known as thermo-oxidative ageing of polymers. Mixing polymeric materials with a complex blend of additives able to inhibit or delay their deterioration is the best way to prevent premature ageing [7]. These additives are named stabilizers, or more commonly antioxidants. They are classified according to their mechanisms of action: primary (AO-I) and secondary (AO-II) antioxidants.

Sterically-hindered phenols (SHP) such as Irganox 1010[®] and Irganox 1076[®], derived from the controversial butylated hydroxytoluene moiety, are the best benchmark antioxidant additives belonging to the AO-I group [7]. They bring oxidative degradation reactions to a close by transferring hydrogen atoms from their phenols to R•, resulting in nonreactive phenoxy radicals. Precisely, SHP act

like radical scavengers thanks to chain-breaking reactions, and thus prevent the formation of R^\bullet , well known to be responsible for polymer degradation [8,9].

Recently, the additive industry has shown increasing interest in naturally occurring *p*-hydroxycinnamic acids (HCAs), such as ferulic, caffeic, sinapic, and *p*-coumaric acids, because of their nontoxic nature yet powerful chain-breaking antioxidative properties, acting through radical scavenging [10–14]. Consequently, we previously reported a library of bisphenolic AO-I derived from HCAs found in lignocellulose (*p*-coumaric, ferulic, and sinapic acids) and biobased diols (1,3-propanediol, 1,4-butanediol, and isosorbide) [15]. To optimize their antiradical activities, we assessed the structure–activity relationships (aka SAR) of these phenolics [16]. The best candidates, obtained from the reaction between ferulic acid and 1,4-butanediol (BDF), 1,3-propane-diol (PDF), or isosorbide (IDF), exhibited potent antioxidant activities competing with commercially available molecules such as Irganox 1010[®]. Their high thermal stabilities (>200 °C) render them compatible with harsh polymer production processes. Furthermore, their molar mass greater than 500 g.mol⁻¹ prevents leaching and other volatility issues. Finally, their eco-friendly preparation makes them an attractive choice as sustainable additives and therefore increases their market value even further. Unfortunately, the polar character of this series of biobased antioxidants leads to a very poor solubility in nonpolar media, such as polyolefins [15]. This major drawback thus limits their reactivity with radicals responsible for oxidation and subsequently reduces their protective role against premature polymer ageing [17]. Indeed, good solubility and mobility have an important positive impact on the stabilization properties of antioxidants [3].

A promising approach to increase compatibility with nonpolar matrix, namely lipophilization, consists in the covalent grafting of lipophilic moieties to phenolics in order to improve both miscibility and incorporation of a given antioxidant in nonpolar media. Lecomte et al. have reported that the grafting of a medium chain-length is the best strategy to design potent lipophilized antioxidants [18]. To date, many of these antioxidants, called phenolipids, have been synthesized from phenolic acid, flavonoids or tocopherols [19–21]. However, the design of these molecules is usually not optimized to provide sustainable alternatives able to challenge commercial additives for polymeric materials in terms of activity, solubility and thermal stability.

This work reports on the design and preparation of new potent sustainable bisphenolics AO-I from lignocellulosic and oleaginous biomasses as we dedicate ourselves to integrated biorefinery concepts. To insure a high antiradical activity, the targeted bisphenolic structures were based on our previously reported structure–activity relationship study (SAR) [15,16] and their solubilities into common polymers were evaluated using Hansen and Hildebrand parameters [22]. Once the structural designs were validated, the chemo-enzymatic synthesis of the target structures was optimized through sustainable chemo-enzymatic processes involving a lipase-catalyzed transesterification strategy [23]. Finally, their activities and thermal stabilities were benchmarked against that of Irganox 1010[®] and lipophilic Irganox 1076[®], two widely used fossil-based antioxidant additives.

2. Experimental

2.1. Materials

Ferulic acid, lauric acid, palmitic acid, stearic acid, glycerol, benzyl bromide, *N,N*-dimethyl-4-aminopyridine (DMAP), and *N,N*-diisopropylcarbodiimide (DIC) were purchased from Sigma-Aldrich (Saint-Louis, MO, USA). *Candida antarctica* Lipase B immobilized on resin (LC200291, 10,000 propyl laurate units g⁻¹) was obtained from Novozyme. Reagents were used as received. All solvents were bought either from ThermoFisher Scientific (Waltham, MA, USA) or VWR France (Fontenay-sous-Bois, France). Deuterated chloroform (CDCl₃) was purchased from Euriso-top (Saint-Aubin, France).

2.2. Analytical Methods

Column chromatography was carried out with an automated flash chromatograph (PuriFlash 4100, Interchim (Montluçon, France), prepacked with INTERCHIM PF-30SI-HP (30 μm silica gel) columns using a gradient of cyclohexane and ethyl acetate for elution. NMR analyses were recorded on a Bruker (Billerica, MA, USA) Fourier 300. ^1H NMR spectra of samples were determined in CDCl_3 at 300 MHz and chemical shifts were reported in parts per million (CDCl_3 , CHCl_3 residual signal at $\delta = 7.26$ ppm). ^{13}C NMR spectra of samples were recorded at 75 MHz (CDCl_3 signal at $\delta = 77.16$ ppm). High-resolution mass spectroscopy (HRMS) analyses were carried out by the PLANET platform at URCA using a Micromass GC-TOF. Thermogravimetric analyses (TGA) were executed on a Q500 (TA Instruments (Milford, MA, USA)). About 10 mg of each sample was heated from 30 to 500 $^\circ\text{C}$ at a rate of 10 $^\circ\text{C min}^{-1}$ under constant nitrogen flow (60 mL min^{-1}).

2.3. Synthesis of Benzylated Ethyl Ferulate

Ethyl ferulate²³ (25 g, 0.1 mol, 1 eq), benzyl bromide (15 mL, 0.12 mol, 1.2 eq), and K_2CO_3 (27 g, 0.2 mol, 2 eq) were dissolved in *N,N*-dimethylformamide (DMF) (0.5 M) and heated to 85 $^\circ\text{C}$. The reaction was monitored by TLC and let run until complete conversion of the starting material (3 h). After cooling to room temperature (r.t.), the mixture was concentrated and filtered to remove K_2CO_3 . The resulting phase was evaporated under reduced pressure and the crude product was purified by flash chromatography on silica gel using cyclohexane and ethyl acetate (90:10) as eluent, providing the desired product as a white powder (32 g, 92%, Figure 1). M.p.: 70.4 $^\circ\text{C}$, ^1H (300 MHz, CDCl_3) δ : 3.90 (3H, s, H_{10}), 5.18 (2H, s, $\text{H}_{\text{CH}_2\text{OBn}}$), 6.30 (2H, d, $J = 15.9$ Hz, H_2), 6.83 to 6.87 (3H, m, $\text{H}_{5,8}$ and 9), 7.30 to 7.35 (5H, m, H_{ArOBn}), 7.62 (2H, d, $J = 15.9$ Hz, H_3), ^{13}C (75 MHz, CDCl_3) δ : 14.4 (C_{12}), 56.0 (C_{10}), 60.4 (C_{11}), 70.8 ($\text{C}_{\text{CH}_2\text{OBn}}$), 110.2 (C_9), 113.3 (C_8), 115.0 (C_2), 122.8 (C_5), 128.1 (C_4), 127.3 to 136.6 (C_{ArOBn}), 145.8 (C_7), 149.8 (C_6), 150.5 (C_3), 167.4 (C_1).

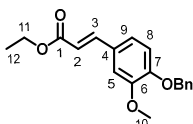


Figure 1. Benzylated ethyl ferulate.

2.4. Lipase-Catalyzed Transesterification of Benzylated Ethyl Ferulate into Glycerol Dibenzyl Ferulate (GDFoBn)

Selective lipase-catalyzed transesterification was performed in presence of glycerol (5 g, 54.3 mmol, 1 eq), benzylated ethyl ferulate (42 g, 135.7 mmol, 2.5 eq) and CAL-B (10% *w/w* relative to the total weight of batch). The reaction mixture was heated to 75 $^\circ\text{C}$, kept under reduced pressure and magnetically stirred for three days. It was then dissolved in acetone and filtered to remove CAL-B beads. The solvent was evaporated under vacuum and the crude product was purified by flash chromatography on silica gel eluted with cyclohexane/ethyl acetate to provide GDFoBn as a highly viscous oil (32 g, 93%, Figure 2). ^1H (300 MHz, CDCl_3) δ : 3.89 (6H, s, H_{10}), 4.22 to 4.39 (4H, m, H_{11}), 4.28 (1H, s, H_{OH}), 5.17 (4H, s, $\text{H}_{\text{CH}_2\text{OBn}}$), 6.30 (2H, d, $J = 15.9$ Hz, H_2), 6.83 to 7.05 (6H, m, $\text{H}_{5,8}$ and 9), 7.25 to 7.40 (10H, m, H_{ArOBn}), 7.61 (2H, d, $J = 15.9$ Hz, H_3), ^{13}C (75 MHz, CDCl_3) δ : 56.0 (C_{10}), 65.4 (C_{11}), 68.6 (C_{12}), 70.8 ($\text{C}_{\text{CH}_2\text{OBn}}$), 110.2 (C_9), 113.3 (C_8), 115.0 (C_2), 122.8 (C_5), 128.14 (C_4), 127.3 to 136.6 (C_{ArOBn}), 145.8 (C_7), 149.8 (C_6), 150.5 (C_3), 167.4 (C_1).

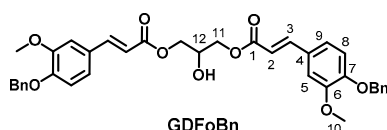


Figure 2. Glycerol dibenzyl ferulate.

2.5. Lipophilization: Synthesis of GDF_x

GDFoBn (20 g, 32.1 mmol, 1 eq) and fatty acid (lauric, palmitic or stearic, 1 eq) were dissolved in dichloromethane (DCM) (0.25 M) with a catalytic amount of DMAP, (1.1 g, 9.6 mmol, 0.3 eq). Subsequently, DIC (5.45 mL, 35.2 mmol, 1.1 eq) was added to the mixture and the reaction was magnetically stirred at r.t. overnight. The precipitate urea was removed via filtration and the filtrate concentrated under vacuum. The crude product was dissolved in THF and stirred under N₂ flow at room temperature. After 10 min, palladium on activated charcoal (Pd/C, 10% *w/w*) was added and the solution was stirred under N₂ for another 10 min, before being submitted to H₂ flow to simultaneously reduce the C=C double bond and the benzyl protecting group (Bn). The solution was finally filtered using Celite® pads and evaporated under reduced pressure. Target bisphenol was purified by flash chromatography on silica gel eluted with cyclohexane/ethyl acetate. Structures were named GDF_x, for Glycerol Diferulate, where the incrementation “x” indicates the alkyl chain length.

GDF₁₀ (84%, Figure 3). ¹H (300 MHz, CDCl₃) δ: 0.87 (3H, t_{app}, J = 6.8 Hz, H₂₄), 1.24 (16H, m, H_{16 to 23}), 1.61 (2H, m, H₁₅), 2.28 (2H, t, J = 7.5 Hz, H₁₄), 2.60 (4H, t, J = 7.6 Hz, H₃), 2.86 (4H, t, J = 7.6 Hz, H₂), 3.79 (6H, s, H₁₀), 4.18 (4H, dd, J = 4.2, 11.7 Hz, H_{11, 11'}), 5.22 (1H, m, H₁₂), 5.53 (2H, s, H_{OH}), 6.65 (2H, s, H₅), 6.68 (2H, s, H₉), 6.81 (2H, d, J = 7.8 Hz, H₈), ¹³C (75 MHz, CDCl₃) δ: 14.2 (C₂₄), 24.9 (C₁₅), 29.1–29.7 (C_{16 to 23}), 30.6 (C₃), 34.2 (C₁₄), 36.1 (C₂), 55.9 (C₁₀), 62.3 (C₁₁), 68.8 (C₁₂), 110.9 (C₉), 114.5 (C₈), 120.9 (C₅), 132.2 (C₄), 144.2 (C₇), 146.5 (C₆), 172.5 (C₁), 173.0 (C₁₃), FT-IR (neat), ν_{max}: 3456 (ArOH), 2922 and 2851 (aliphatic chain), 1733 (C=O), Td_{5%-Loss}: 302 °C, HRMS (TOF MS, ES+): *m/z* calcd for C₃₅H₅₀O₁₀Na: 653.3295; found 653.3302.

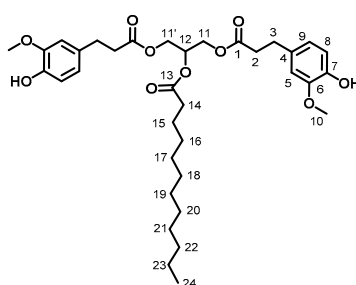


Figure 3. GDF₁₀.

GDF₁₄ (81%, Figure 4). ¹H (300 MHz, CDCl₃) δ: 0.87 (3H, t_{app}, J = 6.3 Hz, H₂₈), 1.23 (24H, m, H_{16 to 27}), 1.59 (2H, m, H₁₅), 2.28 (2H, t, J = 7.5 Hz, H₁₄), 2.61 (4H, t, J = 5.1 Hz, H₃), 2.88 (4H, t, J = 7.5 Hz, H₂), 3.78 (6H, s, H₁₀), 4.17 (4H, dd, J = 4.5, 12.0 Hz, H_{11, 11'}), 5.23 (1H, m, H₁₂), 5.51 (2H, s, H_{OH}), 6.65 (2H, s, H₅), 6.68 (2H, s, H₉), 6.81 (2H, d, J = 7.8 Hz, H₈), ¹³C (75 MHz, CDCl₃) δ: 14.2 (C₂₈), 24.9 (C₁₅), 29.1–29.7 (C_{16 to 27}), 30.6 (C₃), 34.2 (C₁₄), 36.0 (C₂), 55.9 (C₁₀), 62.3 (C₁₁), 68.8 (C₁₂), 110.9 (C₉), 114.5 (C₈), 120.9 (C₅), 132.2 (C₄), 144.2 (C₇), 146.5 (C₆), 172.5 (C₁), 173.0 (C₁₃), FT-IR (neat), ν_{max}: 3460 (ArOH), 2921 and 2850 (aliphatic chain), 1734 (C=O), Td_{5%-Loss}: 311 °C, HRMS (TOF MS, ES+): *m/z* calcd for C₃₉H₅₈O₁₀Na: 709.3937; found 709.3928.

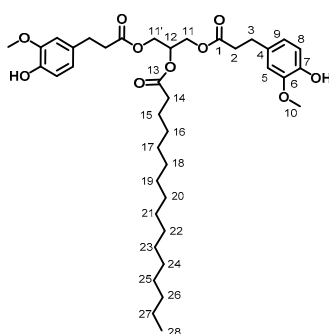


Figure 4. GDF₁₄.

GDF₁₆ (87%, Figure 5). ¹H (300 MHz, CDCl₃) δ: 0.87 (3H, t_{app}, J = 6.3 Hz, H₃₀), 1.24 (28H, m, H_{16 to 30}), 1.58 (2H, m, H₁₅), 2.27 (2H, t, J = 7.5 Hz, H₁₄), 2.60 (4H, t, J = 8.1 Hz, H₃), 2.85 (4H, t, J = 7.5 Hz, H₂), 3.86 (6H, s, H₁₀), 4.17 (4H, dd, J = 4.5, 12.0 Hz, H_{11, 11'}), 5.23 (1H, m, H₁₂), 5.48 (2H, s, H_{OH}), 6.65 (2H, s, H₅), 6.68 (2H, s, H₉), 6.81 (2H, d, J = 7.5 Hz, H₈), ¹³C (75 MHz, CDCl₃) δ: 14.2 (C₃₀), 24.9 (C₁₅), 27.1–29.7 (C_{16 to 29}), 30.6 (C₃), 34.2 (C₁₄), 36.0 (C₂), 55.9 (C₁₀), 62.3 (C₁₁), 68.8 (C₁₂), 110.9 (C₉), 114.5 (C₈), 120.9 (C₅), 132.2 (C₄), 144.2 (C₇), 146.5 (C₆), 172.5 (C₁), 173.0 (C₁₃), FT-IR (neat), ν_{max}: 3454 (ArOH), 2921 and 2850 (aliphatic chain), 1735 (C=O), Td_{5%-Loss}: 308 °C, HRMS (TOF MS, ES+): *m/z* calcd for C₄₁H₆₂O₁₀Na: 737.4252; found 737.4241.

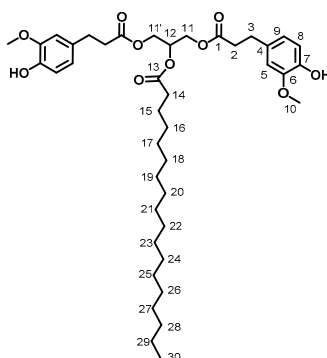


Figure 5. GDF₁₆.

2.6. Calculation of Solubility Parameters

The theoretical solubility and incorporation of additives into polymers were estimated by using the van Krevelen and Hoftyzer atomic group contribution method [22]. The Hansen solubility parameters of compounds were calculated using following equation and the database supplied in electronic supplementary information (ESI).

$$\delta_d = \Sigma F_{di} / \Sigma V_i; \text{ Dispersion component } (J^{1/2} / \text{cm}^{-3/2}) \quad (1)$$

$$\delta_p = \Sigma F_{pi}^2 / \Sigma V_i; \text{ Polar component } (J^{1/2} / \text{cm}^{-3/2}) \quad (2)$$

$$\delta_h = \Sigma E_{hi} / \Sigma V_i; \text{ Hydrogen-bonding component; } (J^{1/2} / \text{cm}^{-3/2}) \quad (3)$$

with

F_{di} : Dispersion contribution of the molar attraction constant $[(J^{1/2} \text{ cm}^{-3/2}) / \text{mol}^{-1}]$

F_{pi} : Polar contribution of the molar attraction constant $[(J^{1/2} \text{ cm}^{-3/2}) / \text{mol}^{-1}]$

E_{hi} : Hydrogen-bonding energy contribution of the molar attraction constant (J/mol)

V : Molar volume contribution of the chemical group involved (cm^3 / mol).

The Hildebrand solubility parameters (HiSP) were then calculated in $J^{1/2} / \text{cm}^{-3/2}$ with the simplified following equation:

$$\text{HiSP} = \sqrt{(\delta_d^2 + \delta_p^2 + \delta_h^2)} \quad (4)$$

2.7. Analysis of the Radical Scavenging Power of Antioxidants

The radical scavenging power was measured with a method derived from Berset et al. [24]. A total amount of 190 μL homogenate DPPH (2,2-diphenyl-1-picrylhydrazyl) ethanol solution (200 μM) was added to a 96-well plate containing 10 μL of potential antiradical molecule ethanol solutions at different concentrations, ranging from 300 μM to 9.3 μM . The experiments were performed in an invariable excess of the DPPH radical (200 μM , 40 nmol). The phenolic concentrations were selected to get linear dose-response intervals. The reaction was followed by a microplate Multiskan FC 1 scan every 5 min for 7.5 h at 515 nm. The use of different amounts of the potential antioxidant gave rise

to the EC_{50} value, which is defined as the concentration needed to reduce half the initial amount of DPPH. Each analysis was performed four times. The total stoichiometries (n) is the number of DPPH moles reduced by 1 mol of antioxidant ($n = DPPH_{tot}/EC_{50} \times 2$).

3. Results and Discussions

3.1. Design of Lipophilic Antioxidants: Predictive Approaches

The design of the new bisphenolic antioxidants was based on our earlier studies on the Structure–Activity Relationships (SAR) of ferulic acid-based diphenolic antioxidants [15]. Ferulic acid is a well-known natural antioxidant because of its hydrogen-donating ability [13,25]. It was shown that removing the α,β -unsaturation was beneficial for the radical-scavenger ability of bisphenolic structures [16]. Therefore, α,β -saturated ferulic acid moieties were selected to confer optimal radical scavenging ability. A previously published SAR study [16] showed that the nature of the linker between the antiradical moieties slightly impacts the antioxidant activity. In this specific study, the linker had to be a triol able to carry the two phenolic moieties as well as an alkyl chain allowing the fine tuning of the lipophilic character of the molecule. Glycerol that carries two primary alcohols and one secondary alcohol was selected. Glycerol is a byproduct during the production of biodiesel, therefore available in high amounts, the use of which helps reduce the environmental impact of this industry [26]. The lipophilic part was based on recent advances, which show that the grafting of a medium chain-length fatty acid can be used to design potent custom-made lipophilic antioxidants [18,21]. Herein, three linear fatty acids were tested. The theoretical miscibility of additives used in the formulation with PP was calculated with the help of the Hildebrand solubility parameters (HiSP, Equation (4)). The lower the difference of HiSP between two compounds, the higher their mutual solubility. In the literature HiSP values in the range between 16.8 and 19.0 $J^{1/2}/cm^{-3/2}$ are reported for PP. The bisphenolics previously developed in our laboratory (i.e., BDF, PDF, and IDF) exhibited HiSP values greater than 25.0 $J^{1/2}/cm^{-3/2}$ (Figure 6, Table 1). Among them, IDF has the highest polarity contribution (δ_p 7.2 vs. 3.5–3.7 $J^{1/2}/cm^{-3/2}$) linked to the polarity of the isosorbide linker. In comparison, benchmark antioxidant Irganox 1010[®] exhibits a low HiSP value of 21.4 $J^{1/2}/cm^{-3/2}$. The commercial lipophilic antioxidant Irganox 1076[®] exhibits a HiSP value much more comparable to that of PP, thanks to a lower contribution of the aliphatic chain to polarity (δ_p) and the other hydrogen bonding (δ_h) factors [27]. The increase of the polar contribution of the target antioxidants was calculated for esters with lauric (C_{12}), palmitic (C_{16}), and stearic (C_{18}) acid. This group of lipophilic antioxidants was named GDF_x , for Glycerol Diferulate, where the incrementation “x” indicates the alkyl chain length. The HiSP values of the GDF_x family were lowered compared to the initial antioxidants, therefore better solubility in PP might be expected (Table 1). The HiSP values showed the importance of alkyl chain length. Indeed, data show that an increase of the chain length by six carbon atoms (GDF_{10} vs. GDF_{16}) leads to a HiSP value drop of 1.00 $J^{1/2}/cm^{-3/2}$ (Table 1).

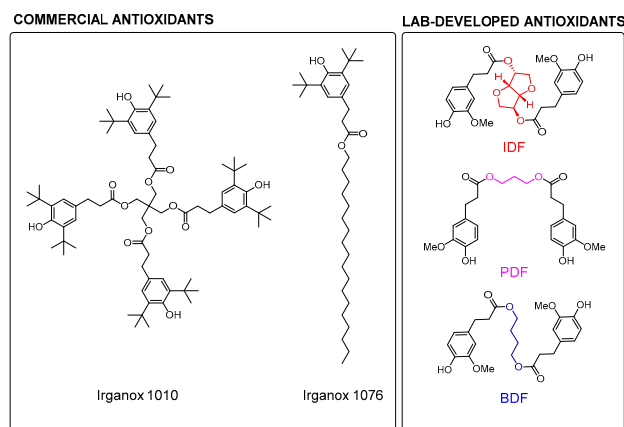


Figure 6. Developed structures of phenolic additives.

Table 1. Hildebrand solubility parameters (HiSP) of phenolic antioxidants.

Compound	δ_d ($J^{1/2} \text{ cm}^{-3/2}$)	δ_p ($J^{1/2} \text{ cm}^{-3/2}$)	δ_h ($J^{1/2} \text{ cm}^{-3/2}$)	HiSP ($J^{1/2} \text{ cm}^{-3/2}$)
BDF	21.3	3.5	13.6	25.5
PDF	21.5	3.7	13.9	25.9
IDF	23.3	7.2	14.9	28.5
GDF ₁₀	19.8	2.5	11.7	23.2
GDF ₁₄	19.5	2.2	10.9	22.5
GDF ₁₆	19.3	2.1	10.7	22.2
Irganox 1010 [®]	18.9	1.3	10.0	21.4
Irganox 1076 [®]	17.4	1.3	7.0	18.8

3.2. Synthesis of the Targets (GDF_x)

As we committed ourselves to the use of sustainable processes for the production of the targeted bisphenols, the use of the previously reported lipase-catalyzed synthesis of IDF, PDF, and BDF was envisaged [23]. Indeed, the use of immobilized lipase CAL-B as a biocatalyst is a great tool for the development of sustainable processes. Not only does CAL-B not require a solvent, it is inactive toward phenolic hydroxyl groups, but can also be reused for further reaction cycles. In addition, CAL-B has been proven to promote the easier (trans)esterification on esters rather than acids moieties. Hence, α,β -saturated ethyl ferulate (aka ethyl dihydroferulate) and fatty acid ethyl ester (FAEE) were selected as starting materials rather than the corresponding acids. Several strategies were investigated to determine the best synthetic pathway to GDF_x. The different pathways (Figure 7) are the

- (I) Stoichiometric one pot-one step enzymatic strategy,
- (II) One pot-two step strategy, and
- (III) Chemo-enzymatic strategy.

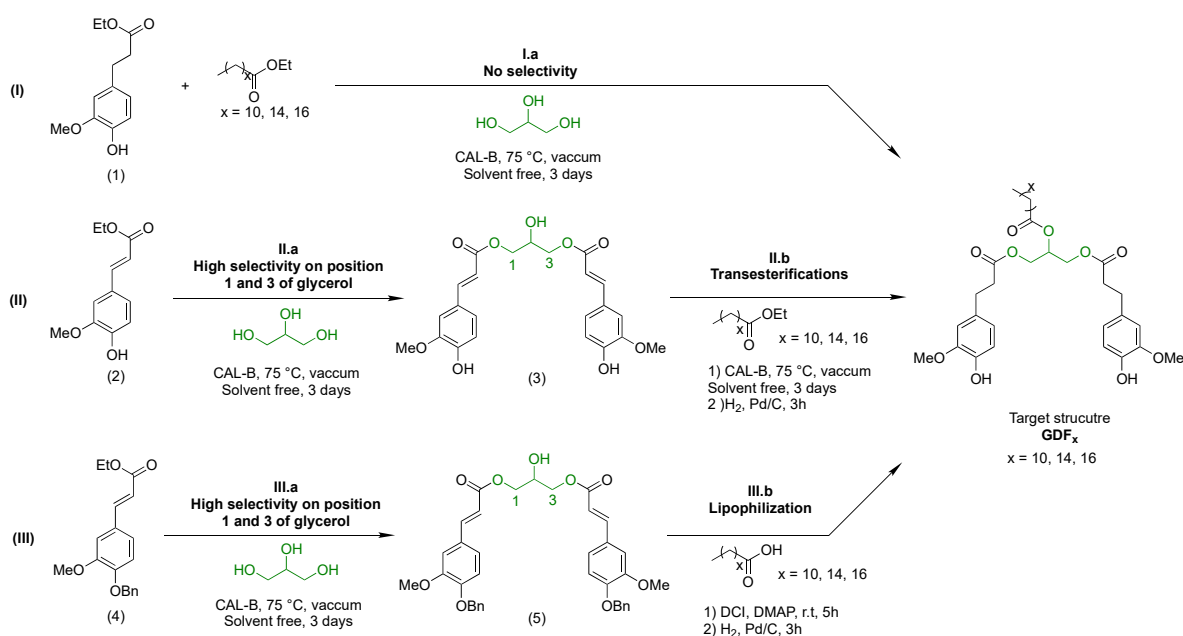


Figure 7. Stoichiometric one pot-one step enzymatic strategy (I), one pot-two step strategy (II), chemo-enzymatic strategy (III), and corresponding yields (I.a: 34%, II.a: 91%, II.b: 40%, III.a: 93%, III.b GDF₁₀: 84%, GDF₁₄: 81%, GDF₁₆: 87%).

3.3. Stoichiometric One Pot-One Step Enzymatic Strategy (Pathway I, Figure 7)

The first strategy (I) involved a one pot-one step lipase-mediated transesterification of glycerol with a mixture of ethyl dihydroferulate (1) (2 eq) and FAEE (1 eq) (I.a—Figure 7). It is worth mentioning that ethyl dihydroferulate can be easily obtained from ethyl ferulate through a simple palladium-catalyzed hydrogenation in yield greater than 98% [23]. Under such stoichiometric conditions, *Candida antarctica* lipase B was not regioselective toward glycerol primary and secondary alcohols. Indeed, despite the total conversion of ethyl dihydroferulate, the enzyme functionalized primary and secondary alcohols randomly with ethyl dihydroferulate or FAEE, leading to a complex mixture of the target structure and corresponding regioisomers. After purification, the targeted GDF_x were isolated in 34% yield.

3.4. One Pot-Two Step Strategy

The transesterification was then performed on α,β -unsaturated ethyl ferulate (2). In that case, *Candida antarctica* lipase B proved unable to esterify the secondary alcohol of glycerol, giving access to the symmetric bisphenol (3) in high yield after purification (II.a, 91%, Figure 7). The α,β -unsaturation of ethyl ferulate (2) conferred probably more rigidity to the molecule and decreased the accessibility to the active site of the lipase. Furthermore, it also decreased significantly the electronic density on the C from the carbonyl, thus limiting its reactivity. With the aim to access GDF_x, a second step involving a lipase-catalyzed transesterification followed by a palladium-catalyzed hydrogenation was then performed on intermediate bisphenol (3) (II.b, Figure 7). This second biocatalytic step induced however transesterification issues due to CAL-B esterase activity, resulting in a complex mixture of regioisomers and therefore in the decrease in yield down to 40% after purification.

3.5. Chemo-Enzymatic Strategy

A protecting group-based chemo-enzymatic strategy was finally developed to produce lipophilic antioxidants in high yields. The first step involved the lipase-mediated transesterification of benzylated ethyl ferulate (4) with the two primary alcohols of glycerol leading to an intermediate bisphenol (5) isolated in 93% yield (III.a, Figure 7). Then, fatty acids were grafted onto the available secondary alcohol through a conventional Steglich esterification, immediately followed by a palladium-catalyzed hydrogenation to simultaneously reduce the α,β -unsaturation and cleave the benzyl protecting group (III.b, Figure 7). Using this third strategy, targeted bisphenols were obtained as single regioisomers in high yields (GDF₁₀: 84%, GDF₁₄: 81%, GDF₁₆: 87%). It is worth mentioning that this synthesis was then successfully implemented on a large scale (≈ 20 g).

The thermal properties of the new additives described in Table 2 were investigated by thermogravimetric analysis (TGA).

Table 2. Thermostability (T_d5%) of GDF_x.

Compound	Thermostability (T _d 5%, °C)
GDF ₁₀	302
GDF ₁₄	311
GDF ₁₆	308
Irganox1076 [®]	236
Irganox1010 [®]	347

Thermogravimetric analyses (TGA) of the bisphenols revealed thermostability (T_d5%) in the range of 302 to 311 °C. Furthermore, the alkyl chain length does not significantly impact the degradation temperature. Indeed, replacing lauric (C₁₂) with palmitic (C₁₆) or stearic (C₁₈) moieties shift their thermostability by less than 10 °C.

3.6. Analysis of the Antiradical Activity of Lipophilic Bisphenols

The DPPH method is an easy and rapid analytical tool to determine the free radical scavenging activity of phenolic compounds and their abilities to quench radicals. [24] The total H atom donation capacities can be evaluated with the EC_{50} value, defined as the quantity of antioxidant (nmol) needed to protonate/quench 50% of the initial population of DPPH. The lower the EC_{50} , the higher the antioxidant activity of a compound is. Because the EC_{50} is intrinsically linked to the structure of the antioxidant, in particular to the number of free phenols, a compound can be also characterized by its antioxidant stoichiometry (n), i.e., the number of DPPH radicals reduced by one molecule of antioxidant [28]:

$$n = \text{DPPH}_{\text{tot}} / EC_{50} \times 2 \quad (5)$$

where DPPH_{tot} is the initial amount of DPPH in nmol.

The principal kinetic parameters of the DPPH reaction are the time needed to reach the steady state at the concentration EC_{50} , i.e., $T_{EC_{50}}$, and the rate of reaction towards free radicals [29]. By combining H atom-donation abilities and kinetic parameters, the Antioxidant Efficiency (AE) [29,30] can be defined in order to characterize the behavior of a substance as antioxidant after:

$$AE = (1/EC_{50}) \times |m(EC_{50})| \quad (6)$$

with $m(EC_{50})$ the slope in the first minutes of the absorbance-versus-time plots at EC_{50} of each compound.

The reaction kinetics of all compounds with DPPH are shown in ESI, and an example of EC_{50} determination can be seen in Figure 8. The reaction proceeds in two stages, with a fast decay in absorbance during the first minutes, followed by a slower one until equilibrium is reached. EC_{50} values and total stoichiometries (n) obtained with the newly synthesized and commercial phenolic additives classified by chemical structure are shown in Table 3.

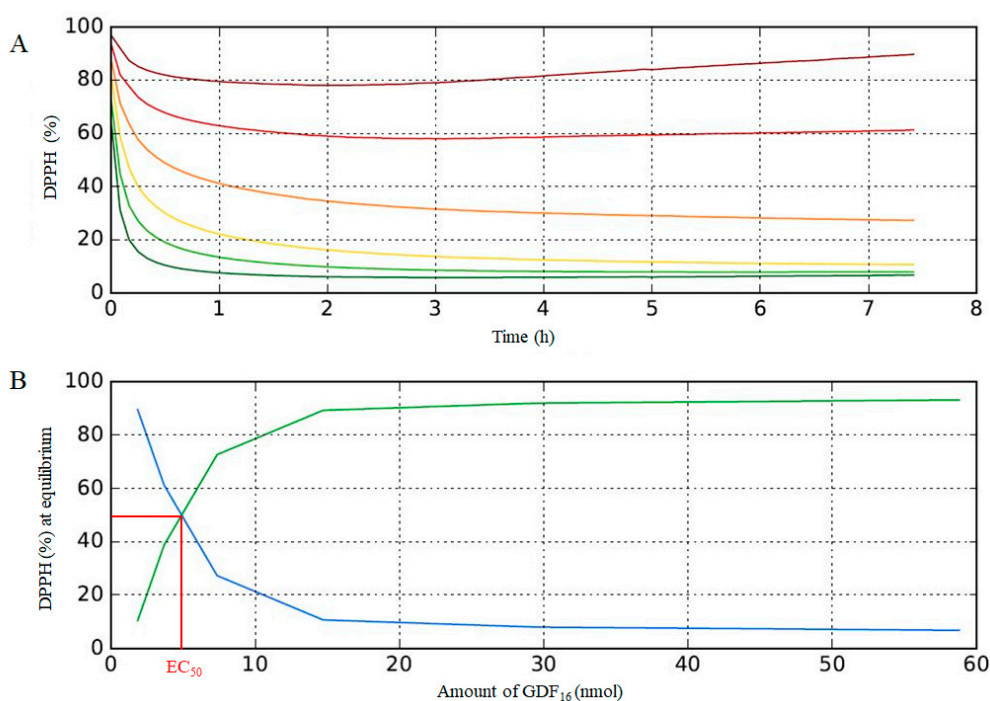


Figure 8. (A) Reaction kinetics of GDF_{16} solution at given concentrations: 300 μM (dark green), 150 μM (light green), 75 μM (yellow), 37.5 μM (orange), 18.8 μM (red), and 9.4 μM (brown), (B) EC_{50} determination for GDF_{16} . Blue line: 2,2-diphenyl-1-picrylhydrazyl (DPPH) radical and Green line: RPPH reduced.

As shown in Table 3, the EC_{50} values for GDF_x are homogenous around 5 nmol (mean value: 4.95 nmol). It is noteworthy to mention that no correlation between the alkyl chains size and the antiradical activity was observed. Irganox 1010[®] is the most potent scavenging compound, whereas Irganox 1076[®] is the least one; GDF_x have intermediate EC_{50} values. The number of phenols available for DPPH quenching is an important feature for the antioxidant activity. Irganox 1010[®] and 1076[®] contains four and one free phenol groups, respectively, while the GDF_x family has only two. The stoichiometries value n takes into account this factor. As expected, with its four phenols, Irganox 1010[®] exhibited an antiradical activity twice as high than that found for the GDF_x family that only bears two phenols. Similarly, the monophenolic compound Irganox 1076[®] displayed an activity twice as low than the bisphenolic compound GDF_x .

Table 3. Radical scavenging parameters of phenolic antioxidants.

Compound	Free Phenols	EC_{50} (nmol)	Stoichiometries (n)	$ m(EC_{50}) $	AE
GDF_{10}	2	4.81 ± 0.17	4.17 ± 0.15	2.19	0.45
GDF_{14}	2	5.38 ± 0.12	3.72 ± 0.09	2.30	0.42
GDF_{16}	2	4.66 ± 0.15	4.30 ± 0.14	2.16	0.46
Irganox 1010 [®]	4	2.52 ± 0.16	7.98 ± 0.47	0.76	0.30
Irganox 1076 [®]	1	11.48 ± 0.17	1.74 ± 0.03	0.68	0.06

The stoichiometry value n does not coincide with the number of hydroxyl groups available. Indeed, the direct abstraction of the phenol H-atom and the electron transfer process from $ArOH$ to DPPH radical is not the only mechanism involved in the reaction between DPPH and phenols. Various studies [31,32] have already proposed potential phenol regeneration pathways leading to reaction products such as dimers or quinone methides, able to further react with DPPH radicals and thus leading to n values higher than 2 (Figure 9).

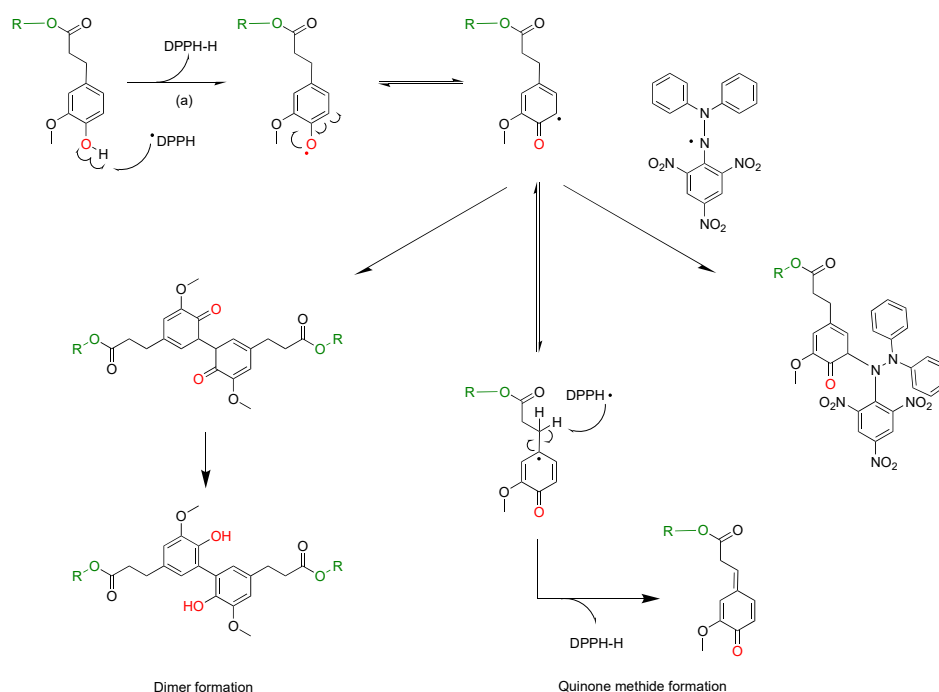


Figure 9. Chemical behavior of phenolic antioxidants.

Finally, in order to determine the antioxidant efficiencies (AE), the absorbance-vs-time plots at the EC_{50} concentration of each phenolic compound were established. When concentration of DPPH was in large excess, the slope in the first minutes of these plots ($m_{EC_{50}} = \Delta y / \Delta x \text{ } 0 \rightarrow 10 \text{ min}$)

could be assimilated to the rate constants of fast reaction of proton abstraction (a) in Figure 9 [29]. Consequently, antioxidant efficiency values (AE) calculated using equation (6) (Table 3 and ESI), take into consideration both H atom-donation capacity and kinetic aspects of the phenolic compounds tested. Here, the higher the AE, the higher the antioxidant activity of a compound is.

Based on these results, the antioxidant Irganox 1076[®] was the least efficient of all tested phenolic compounds. It is interesting to note that a compound such as Irganox 1010[®], with an EC₅₀ value of 2.50, was found to be the best antioxidant of all phenolic compounds, but instead showed a moderate antioxidant efficiency (AE = 0.30), due to its relative slow rate of reaction (Table 3). Finally, the newly created GDF_x family appeared to be competitive showing the highest AE values, ranging from 0.42 to 0.46, due to the combination of high H atom-donation capacities and fast kinetics.

4. Conclusions

A novel class of renewable bisphenol (GDF_x) was successfully designed from ferulic acid and vegetal oil (glycerol and fatty acids) and proved to be potent antioxidant additives for polyolefins. By playing with the chemical structure of the starting materials, their polarities can be easily tuned so to display theoretical solubilities into polypropylene similar to that of Irganox 1010[®]. The efficient synthesis of these novel bisphenols has been achieved through a chemo-enzymatic process involving a highly regioselective lipase-mediated transesterification, allowing the preparation of well structurally defined targets in very good yields (81–87%). The H atom-donation capacities and kinetic aspects of these novel bisphenols were evaluated using the DPPH free radical technique and benchmarked against commercially available antioxidant compounds. All of the results demonstrated the high radical scavenging capacity of these renewable bisphenols and their potential as promising renewable alternatives. The study of their antioxidant capacity in polyolefins matrices will be reported in due course.

Supplementary Materials: The following are available online at <http://www.mdpi.com/1422-0067/19/11/3358/s1>.

Author Contributions: Conceptualization, F.A.; Methodology, L.H., F.A.; Validation, S.D. and F.A.; Formal Analysis, L.H.; Investigation, L.H. and F.A.; Resources, F.A.; Data Curation, L.H.; Writing-Original Draft Preparation, L.H.; Writing-Review & Editing, S.D. and F.A.; Supervision, S.D. and F.A.; Project Administration, F.A.; Funding Acquisition, F.A.

Funding: This research was funded by Grand Reims, Conseil Général de la Marne and Région Grand Est.

Acknowledgments: The authors are grateful to Grand Reims, the Conseil Général de la Marne and Région Grand Est for their financial support.

Conflicts of Interest: The authors declare no conflict of interest.

References

1. Zweifel, H. *Stabilization of Polymeric Materials*; Springer: New York, NY, USA, 1998.
2. Zweifel, H. *Polymer Durability: Degradation, Stabilization, and Lifetime Prediction*; ACS Publishing: New York, NY, USA, 1996.
3. Scott, G. *Polymer Degradation and Stabilisation*; Cambridge University Press: Cambridge, UK, 1988.
4. Sohma, J. Mechano-radical formation in polypropylene by an extruder action and its after-effects. *Colloid Polym. Sci.* **1992**, *270*, 1060–1065. [[CrossRef](#)]
5. Verdu, J. *Oxydative Ageing of Polymers*; John Wiley & Sons: Hoboken, NJ, USA, 2012.
6. Bolland, J.L.; Gee, G. Kinetic studies in the chemistry of rubber and related materials. III. Thermochemistry and mechanisms of olefin oxidation. *Trans. Faraday Soc.* **1946**, *42*, 244–252. [[CrossRef](#)]
7. Pritchard, G. *Plastics Additives: An A-Z Reference*; Polymer Science and Technology Series; Springer: Haarlem, The Netherlands, 2012.
8. Pospíšil, J.; Klemchuk, P.P. *Oxidation Inhibition in Organic Materials*; Taylor & Francis: Abingdon, UK, 1989.
9. Pospíšil, J. Chemical and photochemical behaviour of phenolic antioxidants in polymer stabilization: A state of the art report, part II. *Polym. Degrad. Stab.* **1993**, *39*, 103–115. [[CrossRef](#)]

10. Brewer, M. Natural antioxidants: Sources, compounds, mechanisms of action, and potential applications. *Compr. Rev. Food Sci. Food Saf.* **2011**, *10*, 221–247. [[CrossRef](#)]
11. Dimitrios, B. Sources of natural phenolic antioxidants. *Trends Food Sci. Technol.* **2006**, *17*, 505–512. [[CrossRef](#)]
12. Gaspar, A.; Martins, M.; Silva, P.; Garrido, E.M.; Garrido, J.; Firuzi, O.; Miri, R.; Saso, L.; Borges, F.J. Dietary phenolic acids and derivatives. Evaluation of the antioxidant activity of sinapic acid and its alkyl esters. *Agric. Food Chem.* **2010**, *58*, 11273–11280. [[CrossRef](#)] [[PubMed](#)]
13. Kikuzaki, H.; Hisamoto, M.; Hirose, K.; Akiyama, K.; Taniguchi, H.J. Antioxidant properties of ferulic acid and its related compounds. *Agric. Food Chem.* **2002**, *50*, 2161–2168. [[CrossRef](#)]
14. Gülçin, I. Antioxidant activity of caffeic acid (3,4-dihydroxycinnamic acid). *Toxicology* **2006**, *217*, 213–220. [[CrossRef](#)] [[PubMed](#)]
15. Reano, A.F.; Domenek, S.; Pernes, M.; Beaugrand, J.; Allais, F. Ferulic acid-based bis/trisphenols as renewable antioxidants for polypropylene and poly(butylene succinate). *ACS Sustain. Chem. Eng.* **2016**, *4*, 6562–6571. [[CrossRef](#)]
16. Reano, A.F.; Chérubin, J.; Peru, A.M.M.; Wang, Q.; Clément, T.; Domenek, S.; Allais, F. Structure–activity relationships and structural design optimization of a series of *p*-hydroxycinnamic acids-based bis-and trisphenols as novel sustainable antiradical/antioxidant additives. *ACS Sustain. Chem. Eng.* **2015**, *3*, 3486–3496. [[CrossRef](#)]
17. Pouteau, C.; Dole, P.; Cathala, B.; Averous, L.; Boquillon, N. Antioxidant properties of lignin in polypropylene. *Polym. Degrad. Stab.* **2003**, *81*, 9–18. [[CrossRef](#)]
18. Cruz Figueroa-Espinoza, M.; Laguerre, M.; Villeneuve, P.; Lecomte, J. From phenolics to phenolipids: Optimizing antioxidants in lipid dispersions. *Lipid Technol.* **2013**, *25*, 131–134. [[CrossRef](#)]
19. Figueroa-Espinoza, M.-C.; Villeneuve, P. Phenolic acids enzymatic lipophilization. *J. Agric. Food Chem.* **2005**, *53*, 2779–2787. [[CrossRef](#)] [[PubMed](#)]
20. Jakovetić Tanasković, S.; Jokić, B.; Grbavčić, S.; Drvenica, I.; Prlainović, N.; Luković, N.; Knežević-Jugović, Z. Immobilization of *Candida antarctica* lipase B on kaolin and its application in synthesis of lipophilic antioxidants. *Appl. Clay Sci.* **2017**, *135*, 103–111. [[CrossRef](#)]
21. Laguerre, M.; Bayrasy, C.; Lecomte, J.; Chabi, B.; Decker, E.A.; Wrutniak-Cabello, C.; Cabello, G.; Villeneuve, P. How to boost antioxidants by lipophilization? *Biochimie* **2013**, *95*, 20–26. [[CrossRef](#)] [[PubMed](#)]
22. Van Krevelen, D.W.; te Nijenhuis, K. *Properties of Polymers: Their Correlation with Chemical Structure; Their Numerical Estimation and Prediction from Additive Group Contributions*; Elsevier Science: Amsterdam, The Netherlands, 2009.
23. Pion, F.; Reano, A.F.; Ducrot, P.-H.; Allais, F. Chemo-enzymatic preparation of new bio-based bis-and trisphenols: New versatile building blocks for polymer chemistry. *RSC Adv.* **2013**, *3*, 8988–8997. [[CrossRef](#)]
24. Brand-Williams, W.; Cuvelier, M.E.; Berset, C. Use of a free radical method to evaluate antioxidant activity. *LWT Food Sci. Technol.* **1995**, *28*, 25–30. [[CrossRef](#)]
25. Graf, E. Antioxidant potential of ferulic acid. *Free Radic. Biol. Med.* **1992**, *13*, 435–448. [[CrossRef](#)]
26. Mario, P.; Rosaria, C.; Hiroshi, K.; Michele, R.; Cristina, D.P. From glycerol to value-added products. *Angew. Chem. Int. Ed.* **2007**, *46*, 4434–4440.
27. Reano, F.A. *L'acide Férulique et la (Bio-)Catalyse: Un Tandem Efficace pour la Production de Nouveaux Antioxydants Polyphénoliques*; Ecole Doctorale ABIES AgroParisTech: Paris, France, 2016.
28. Bondet, V.; Brand-Williams, W.; Berset, C. Kinetics and mechanisms of antioxidant activity using the DPPH. free radical method. *LWT Food Sci. Technol.* **1997**, *30*, 609–615. [[CrossRef](#)]
29. Villaño, D.; Fernández-Pachón, M.S.; Moyá, M.L.; Troncoso, A.M.; García-Parrilla, M.C. Radical scavenging ability of polyphenolic compounds towards DPPH free radical. *Talanta* **2007**, *71*, 230–235. [[CrossRef](#)] [[PubMed](#)]
30. Scherer, R.; Godoy, H.T. Antioxidant activity index (AAI) by the 2,2-diphenyl-1-picrylhydrazyl method. *Food Chem.* **2009**, *112*, 654–658. [[CrossRef](#)]
31. Pospíšil, J.; Nešpířek, S.; Zweifel, H. The role of quinone methides in thermostabilization of hydrocarbon polymers—I. Formation and reactivity of quinone methides. *Polym. Degrad. Stab.* **1996**, *54*, 7–14. [[CrossRef](#)]
32. Pospíšil, J. Mechanistic action of phenolic antioxidants in polymers—A review. *Polym. Degrad. Stab.* **1988**, *20*, 181–202. [[CrossRef](#)]



© 2018 by the authors. Licensee MDPI, Basel, Switzerland. This article is an open access article distributed under the terms and conditions of the Creative Commons Attribution (CC BY) license (<http://creativecommons.org/licenses/by/4.0/>).